The application of MRI pulse sequences in the verification of proton beam radiotherapy

J. Seco[1], R. T. Seethamraju[2], G. P. Broussard[3], H. Kooy[1], and M. Harisinghani[4]

[1]Radiation Oncology, Harvard Medical School and Massachusetts General Hospital, Boston, MA, United States, [2]Siemens Medical Solutions, USA Inc., Charlestown, MA, United States, [3]Francis H Burr Proton Center, Massachusetts General Hospital, Boston, MA, United States, [4]Radiology, Harvard Medical School and Massachusetts General Hospital, Boston, MA, United States

Introduction

The purpose of this study is to assess the clinical feasibility and effectiveness of magnetic resonance imaging (MRI) for quality assurance in proton beam therapy. The hypothesis is that as MRI relies on the relaxation times of protons within the patient and proton beam therapy delivers protons to the tumor volume, the extra protons delivered to the cancer tumor volume will produce an additional magnetic signal that can be observed by MRI. The principal advantage of proton radiation over other widespread radiation techniques in cancer therapy is the finite range of protons in the patient, known as the Bragg peak. But in most patients the precise position to stop the proton beam is not exactly known because of organ motion (lung cancer), patient setup error or/and bone structures in the beam (skull in brain cancer). Proton range uncertainties or/and motion variations can be on the order of several centimeters, significantly reducing the benefit of proton therapy because of the excessive amount of radiation given to health tissues surrounding the cancer tumor. In addition, because protons are completely stopped in the patient, no conventional monitoring methods like electronic portal imaging can be applied. Therefore, MRI is assessed as a tool to give functional information of proton beam therapy of cancerous tumor volume.

Materials and Methods

Being that magnetic field changes are produced in the lattice within the tumor or surrounding tissue by the therapeutic proton irradiation, dedicated MR pulse sequences were used to produce an images of the location of these extra protons and their electromagnetic disturbance. A 1.5 Tesla MRI machine was used in the present study. Several gel and animal tissue phantoms were made to assess the feasibility of the MRI to quantitatively and qualitatively capture the additional therapeutic protons. In figure 1, we show the experimental setup of the treatment. The protons have a finite range in the gel/tissue, where the majority of the protons accumulate at the end of the range (represented in the figure by the RED arrow). The gel phantoms were composed of either gelatin (high content of water) or mayonnaise (high content of fatty compounds). The tissue phantom was composed of bovine tissue with muscle and fat. The proton beams used had a range of approximately 16 cm in water (corresponds approximately to 160 MeV kinetic energy) and modulation of 6 cm. A total dose of 500 cGray was delivered to each phantom, which took a total of 5 minutes. Each phantom was imaged with dedicated T1, T2 and T2* weighted MR sequences 5-10 minutes post-proton irradiation.

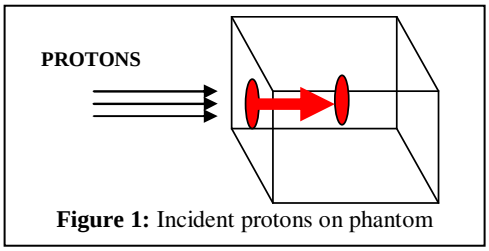

Figure 1: Incident protons on phantom

Results

Preliminary results obtained with gelatin and mayonnaise phantoms are presented in figures 2&3. In figure 2 a T1 (3D VIBE) image (TE=2.45ms and TR=5.27ms) of the gelatin produced a bright oval region representing the end of range of the proton treatment. The signal is generated by the extra protons associated with the proton irradiation beam. The gelatin phantom is very homogeneous and therefore is possible to predict the range of the protons within the phantom. In the present study the range observed was of the order of 5 cm.

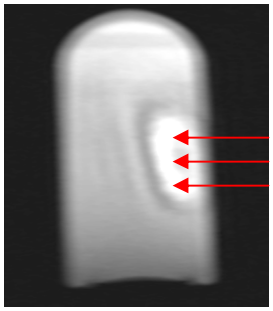

Figure 2: T1 image of gelatin phantom with bright white spot the incident proton beam.

In figure 3, a T2* (GRE) image (TE=48ms and TR=2200ms) is produced for the mayonnaise phantom where the large bright area in the phantom represents the broad proton beam irradiating the phantom. However, since the mayonnaise phantom was not very homogeneous the protons within the phantom were unable to produce a flat end of range (represented by the yellow line). Some variations exist around the end of range due to air pockets within the mayonnaise phantom that affect the motion of the protons in the phantom.

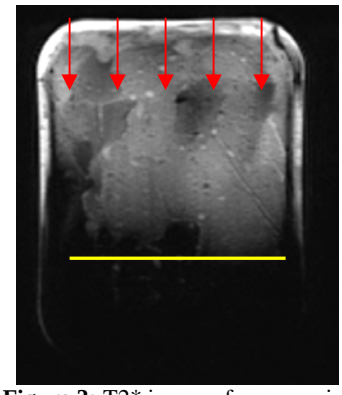

Figure 3: T2* image of mayonnaise phantom with bright white region the incident proton beam.

Discussion

Currently for this abstract we have restricted to qualitative evaluation of the end of range treatment, though all sequences used for this experiment produce quantitative maps for T1, T2 and T2* values. We are in the process of evaluating the quantitative images for the effect the protons have on specific tissue types in the area of irradiation. This could potentially answer the therapeutic aspects of the treatment also.

Conclusion

We have demonstrated the MRI imaging can be used in proton radiation therapy to measure the end of range of a treatment. This observation has profound implications to proton radiotherapy quality assurance since it will allow in-vivo verification of proton therapy.